



ARTICLE

Molecular Cloning, Subcellular Localization and Expression Analyses of *PdbHLH57* Transcription Factor in Colored-Leaf Poplar

Yuhang Li¹, Li Sun¹, Tao Wang¹, Bingjun Yu², Zhihong Gao³, Xiaochun Shu¹, Tengyue Yan¹, Weibing Zhuang^{1,2,*} and Zhong Wang^{1,*}

¹Jiangsu Key Laboratory for the Research and Utilization of Plant Resources, Institute of Botany, Jiangsu Province and Chinese Academy of Sciences (Nanjing Botanical Garden Mem. Sun Yat-Sen), Nanjing, 210014, China

²College of Life Sciences, Nanjing Agricultural University, Nanjing, 210095, China

³College of Horticulture, Nanjing Agricultural University, Nanjing, 210095, China

*Corresponding Authors: Weibing Zhuang. Email: weibingzhuangnj@sina.com; Zhong Wang. Email: wangzhong19@163.com

Received: 20 January 2025; Accepted: 13 March 2025; Published: 30 April 2025

ABSTRACT: bHLH transcription factors, widely exist in various plants, and are vital for the growth and development of these plants. Among them, many have been implicated in anthocyanin biosynthesis across various plants. In the present study, a *PdbHLH57* gene, belonging to the bHLH IIIf group, was characterized, which was isolated and cloned from the colored-leaf poplar ‘Zhongshancai Yun’ (ZSCY). The cDNA sequence of *PdbHLH57* was 1887 base pairs, and the protein encoded by *PdbHLH57* had 628 amino acids, the isoelectric point and molecular weight of which were 6.26 and 69.75 kDa, respectively. Through bioinformatics analysis, *PdbHLH57* has been classified into the IIIf bHLH subgroup, with many members of this subgroup known to participate in anthocyanin biosynthesis. The subcellular localization analysis conducted in the leaf protoplasts of ‘ZSCY’ revealed that the *PdbHLH57* protein is specifically localized in the nucleus. The transcription activation analysis was also conducted, and the results showed that the *PdbHLH57* protein had self-transcription activation. To better explore the functions of the *PdbHLH57* protein, two parts of this protein (*PdbHLH57*-1, *PdbHLH57*-2) were split to detect their transcriptional activation activity. The results indicated that *PdbHLH57*-1 (1-433aa) had self-transcription activation, and *PdbHLH57*-2 (433-628aa) had no transcription activation. The expression of *PdbHLH57* peaked in June during different developmental stages in ‘ZSCY’, and it was most highly expressed in the phloem among various tissues. These findings offer a basis for understanding the role of *PdbHLH57* in colored-leaf poplar.

KEYWORDS: Transcription factors; *PdbHLH57*; subcellular localization; transcription activation analysis; expression pattern; colored-leaf poplar

1 Introduction

Colored-leaf plants have emerged as significant components of modern landscapes due to their tripartite value in socio-economic development, environmental sustainability, and aesthetic enhancement. Colored-leaf poplars, as part of this group, offer numerous advantages such as superior quality, strong adaptability, and high disease resistance, making them widely utilized for courtyard decoration and roadside greenery [1–3]. Recently, several varieties of colored-leaf poplars have been developed, including ‘Quanhong Poplar’ (QHP), ‘Jinhong Poplar’ (JHP), ‘Zhongshancai Yun’ (ZSCY), ‘Caihong Poplar’ (CHP), and ‘Zhonghong Polar’ (ZHP) [4–6]. Among these colored-leaf poplars, ‘ZSCY’ has been widely used due to its rich and unique



colors and longer ornamental period. However, the pathways of pigment formation in ‘ZSCY’ are not yet understood. Consequently, it is crucial to explore the molecular mechanisms of pigment formation in ‘ZSCY’.

Transcription factors (TFs) serve as master regulators of plant growth, development, and environmental adaptation, orchestrating processes ranging from signaling to secondary metabolism. Plant bHLH transcription factors are a large family of transcription factors characterized by a basic helix-loop-helix (bHLH) domain. This domain enables them to bind to specific DNA sequences and regulate the expression of target genes. Besides the bHLH domain, the overall consensus amino acid sequence between bHLH proteins is poorly conserved. This is partly because of the presence of additional domains necessary to modulate their activity and/or DNA-binding specificity, such as the leucine-zipper motif, the MYB-interacting region (MIR), or the aspartate kinase, chorismate mutase, and TyrA-like (ATC-like) domain [7,8]. Many bHLH transcription factors have been identified in various species, which play important roles in various aspects of plant growth and development, such as cell differentiation, development, and responses to environmental stresses. In *Arabidopsis*, more than 162 members of bHLH proteins have been identified, which were further clustered into 12 distinctive subfamilies [8]. Among them, IIIf subfamily bHLH members might be involved in flavonoid biosynthesis, such as *AtbHLH0012/MYC1* and *AtbHLH042/TT8* [9]. More and more bHLH TF associated with flavonoid synthesis have been identified [9,10]. *Lc* in maize was the first plant bHLH TF associated with flavonoid synthesis [11]. In the Asiatic hybrid lily (*Lilium spp.*), *LhbHLH2* has been shown to play a role in the anthocyanin biosynthesis of lily buds when they suffer from light [12]. *MdbHLH3*, isolated from apple (*Malus domestica* Borkh.), promoted fruit coloration and the accumulation of anthocyanin when they were exposed to low temperatures [13]. *CmbHLH2*, clustered in the IIIf bHLH subgroup, could combine with the promoter of *CmDFR* to enhance the accumulation of anthocyanin when co-expressed with *CmMYB6* in chrysanthemum (*Chrysanthemum morifolium* Ramat.) [14]. *FcbHLH42*, a gene isolated from fig (*Ficus carica* L.), was transiently expressed in tobacco, leading to a noticeable accumulation of anthocyanins [15]. AcB2, one of the IIIf bHLH subfamily members, could cooperate and physically interact with AcMYB1 to regulate the expression levels of structural genes associated with anthocyanin biosynthesis, including *AcANS* and *AcF3H1*, which increased the accumulation of anthocyanins in onion (*Allium cepa* L.) [16]. However, fewer bHLH TFs related to the accumulation of anthocyanins have been discovered in poplar. *PdTT8* could significantly enhance the expression level of anthocyanin biosynthesis genes, which were isolated from *Populus deltoids* [17]. In poplar (*Populus trichocarpa*), bHLH131 could form the MBW complex with another two TF (PtrMYB57 and PtrTTG1), which could bind to the promoter of flavonoid genes, such as *ANS1*, *DFR1*, *CHS4*, and *4CL5*, thereby inhibiting the biosynthesis of anthocyanin [18]. In the future, more bHLH TFs related to the biosynthesis of anthocyanin need to be identified.

In our previous study, the anthocyanin contents between green-leaf poplar and colored-leaf poplar were determined, and the genome-wide identification and characterization of PdbHLH transcription factors in colored-leaf poplar were also conducted. Combined with the transcriptome analysis between green-leaf poplar and colored-leaf poplar, *PdbHLH57* from subgroup III(f) might be involved in anthocyanin biosynthesis [19]. However, the functional and structural characterization of this gene remains unclear. In this experiment, *PdbHLH57* was isolated from the leaves of ‘ZSCY’, and structural and functional analysis was conducted to obtain the basic information of *PdbHLH57*. The transcriptional activation assay and subcellular localization analysis were also conducted. Additionally, the expression pattern of *PdbHLH57* was evaluated in poplar leaves at 2-month intervals from 15 April to 15 October 2023. The spatial expression pattern of *PdbHLH57* in ‘ZSCY’ was also explored, including immature leaves, mature leaves, petioles, phloem, xylem, and roots. In addition, anthocyanin contents of ‘ZSCY’ leaves at different developmental stages were measured. The results acquired in the present study could establish some foundations to better analyze functions of *PdbHLH57* in poplar.

2 Materials and Methods

2.1 Plant Material

The deciduous colored-leaf poplar cultivar ‘ZSCY’ used in the present study was cultivated at Nanjing Botanical Garden Mem. Sun Yat-Sen. The leaf color of ‘ZSCY’ is dark red (RHS 47B) in spring, while the leaf color of the upper leaves was RHS 67B; the middle and lower leaves were RHS 189C and RHS N189B in summer. Field management practices such as irrigation and fertilization were conducted according to common practices. Leaves of ‘ZSCY’ were collected at 2-month intervals from 15 April to 15 October 2023. Specific tissues (young leaves, mature leaves, petioles, phloem, xylem, and roots) were harvested on 15 June 2024. The experiments were conducted with three biological replicates, each consisting of three technical replicates. Collected samples were immediately frozen in liquid nitrogen and stored at -80°C for subsequent analyses.

2.2 Total RNA Extraction and cDNA Synthesis

Total RNA was extracted from ‘ZSCY’ leaves using a commercial RNA extraction kit. RNA quality was assessed by 1% agarose gel electrophoresis, with quantification performed using a NanoDrop 2000 spectrophotometer. First-strand cDNA was synthesized using the PrimeScript™ RT Reagent Kit (RR047A, Dalian, China) following manufacturer’s protocols.

2.3 Identification and Cloning of *PdbHLH57*

The cDNA template from ‘ZSCY’ leaves was used to obtain the sequence of the *PdbHLH57* gene with specific primers (Table S1). The reference sequences of *PdbHLH57* were acquired from the database of Phytozome, and SnapGene software was used to design primers. Polymerase chain reaction was used to amplify the ORF sequence of *PdbHLH57* in ‘ZSCY’ leaves. The products obtained were subsequently purified and subcloned into a vector with different kits (FastPure Gel DNA Extraction Mini Kit and pTOPO001 Blunt Simple Vector). Successfully converted monoclonal antibodies were used to be sequenced by GeneralBiol (Anhui, China).

2.4 Gene Structure and Bioinformatics Analysis of *PdbHLH57*

The online tool ProtParam was used to calculate the theoretical isoelectric point and molecular weight. The subcellular localization of *PdbHLH57* was predicted with the online tool CELLO. The sequence alignments between *PdbHLH57* protein and other bHLH proteins were conducted with the software DNAMAN, and these sequences can be downloaded from the database of Arabidopsis Information Resource (TAIR) and National Center for Biotechnology Information (NCBI). With neighbor-joining (NJ) method in MEGA11 software, phylogenetic trees were built using 1000 bootstrap replicates. The prediction of transmembrane domain in *PdbHLH57* protein was carried out by the online tool TMHMM. The online tool STRING was used to predict the interaction network of candidate genes with option value >0.400 . The online tools PSIPRED and Phyre2 were used to predict secondary structure and tertiary structure of *PdbHLH57*.

2.5 Subcellular Localization of *PdbHLH57*

The coding sequences of *PdbHLH57* were cloned into pAN580 vector with specific primers (Table S1) to obtain *PdbHLH57*-GFP construct, which was driven by the double 35S promoter, and included a GFP tag to detect its subcellular localization. Protoplast preparation and transformation were carried out by a previously established method with some modification [20]. The protoplasts used for introducing the *PdbHLH57*-GFP construct were generated from tender leaves of ‘ZSCY’. Before examination, the protoplasts used for

introducing the PdbHLH57-GFP construct were incubated for 16 h at 28°C. The confocal laser scanning microscope (LSM980, Carl Zeiss, Oberkochen, Germany) was used to determine the subcellular localization of PdbHLH57, and the emission wavelength and excitation wavelength used to record their GFP signals were 509 and 488 nm, respectively.

2.6 Transcriptional Activation Assay of PdbHLH57

According to the manual instructions, Matchmaker[®] Gold Yeast Two-Hybrid System was used to determine the transcriptional activity of PdbHLH57 (Clontech, Mountain View, CA, USA). The different parts of PdbHLH57 sequences (1–628 aa, PdbHLH57; 1–425 aa, PdbHLH57-1; 426–628 aa, PdbHLH57-2) were independently fused in the pGBKT7 vector with a GAL4 DNA-binding region, and these fused pGBKT7 vectors were introduced into the yeast strain Y2H. In addition, the co-transformation between pGADT7-T and pGBKT7-Lam served as negative control, while the co-transformation between pGADT7-T and pGBKT7-53 served as positive control. The transformants were incubated for 3–5 days at 30°C, and the activity of transcriptional activation was evaluated on the selective solid medium plate SD/–Trp, supplemented with 200 ng/mL AbA. The presence of blue colonies on the selective solid medium plate indicated the candidate proteins had a self-transactivation activity in yeast cells.

2.7 Anthocyanin Content Measurement

The contents of ‘ZSCY’ leaves anthocyanin were determined with a previous method with some modification [6]. The fresh leaves (about 1.0 g) were placed into 10 mL ethanol mixture with 1% HCl (v/v), which was maintained 30 min at 60°C. The supernatant was collected after centrifuging the mixture for 5 min at 13,000× g, and the absorbance of the supernatant was measured using a spectrophotometer at 650, 620, and 530 nm. The contents of anthocyanin were calculated using the formula $[(A_{530} - A_{620} - 0.1 \times (A_{650} - A_{620})) \times 2500/0.462]$ per gram of fresh weight, and the unit of anthocyanin content was $\mu\text{g/g}$ fresh weight.

2.8 Tissue Specificity and Spatial Specificity of Expression

To better understand the function of *PdbHLH57*, the expression level of *PdbHLH57* at different growth stages and in various tissues of ‘ZSCY’ including young leaves, mature leaves, petioles, phloem, xylem and roots were further evaluated. The procedure and data analysis of qTR-PCR were conducted by the previous method [21]. Primers used in the study were listed in Table S1, and *Actin2*, *EF1* and *UBQ* genes were used as reference genes [22].

3 Results

3.1 Cloning of PdbHLH57 in ‘ZSCY’ Leaves and Sequence Analysis

The sequences of *PdbHLH57* were obtained in the leaves of ‘ZSCY’ with the specific primers (Table S1). An expected band was amplified by RT-PCR using the cDNA of ‘ZSCY’ leaves, which was 1887 bp in length encoded 628 amino acids (Fig. S1, Table S3). According to the bioinformatics analysis, the *PdbHLH57* protein had an Mw of 69.75 kDa, and the pI was 6.26. In addition, the *PdbHLH57* protein also contained a typical bHLH domain (Fig. 1a).

A neighbor-joining phylogenetic tree between PdbHLH57 and other bHLH proteins from other plants was constructed using MEGA 11 software. The results showed that there was a close relationship between PdbHLH57 and AtGL3, AtEGL3, which belonged to the subgroup bHLH IIIif family involved with anthocyanin biosynthesis (Fig. 1b).

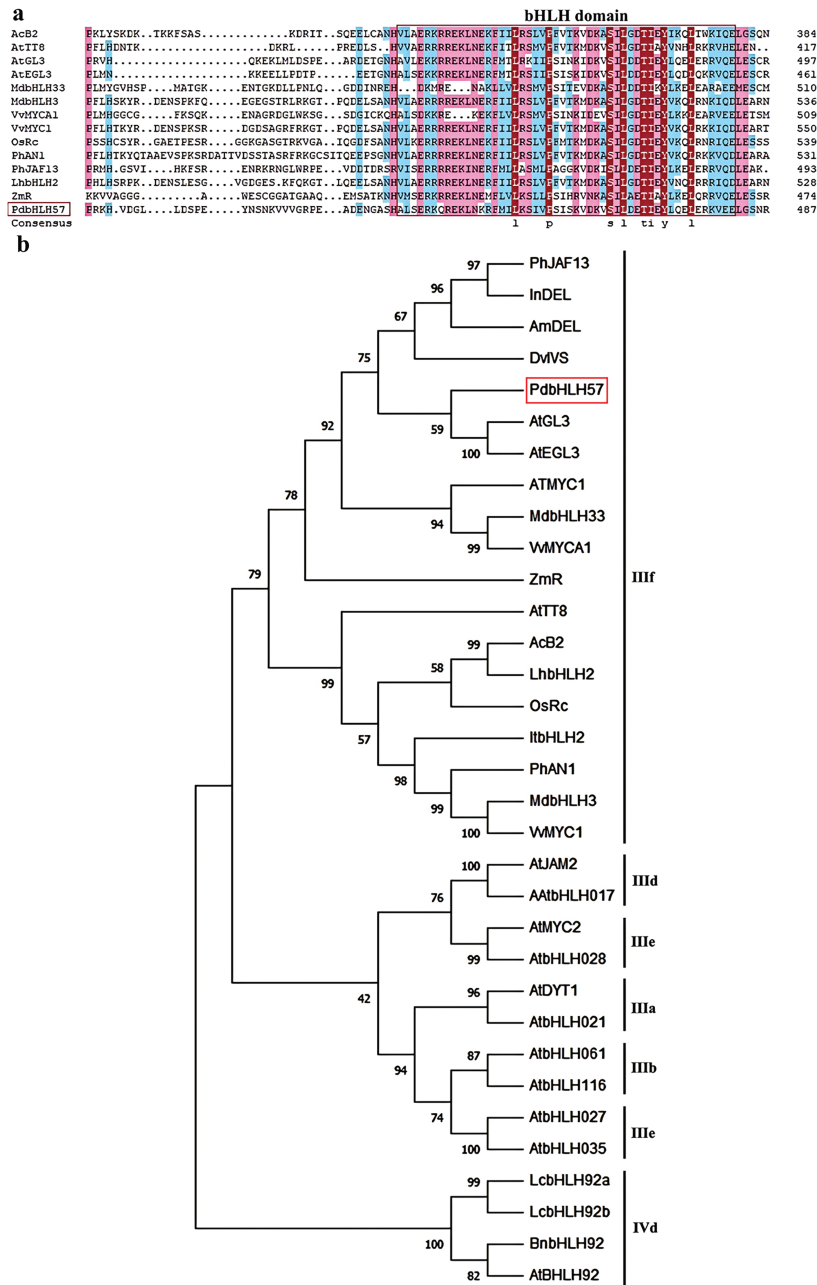


Figure 1: Protein sequence alignment and phylogenetic analysis between PdbHLH57 in ‘ZSCY’ and other bHLH proteins from other plants. The other bHLH proteins are as follows: *Arabidopsis thaliana* AtTT8 (Q9FT81), AtGL3 (NP_680372), AtEGL3 (Q9CAD0), AtMYC1 (BAA11933), AtbHLH061 (AAM10950), AtbHLH116 (AAL84972), AtDYT1 (O81900), AtbHLH021 (NP_179283), AtbHLH027 (AAS79544), AtbHLH035 (NP_974948), AtJAM2 (Q9LNJ5), AtbHLH017 (AAM19778), AtMYC2 (Q39204), and AtbHLH028 (AAL55721); *Malus domestica* MdbHLH33 (ABB84474) and MdbHLH3 (ADL36597); *Vitis vinifera* VvMYCA1 (ABM92332) and VvMYC1 (ACC68685); *Medicago truncatula* MtTT8 (KM892777); *Oryza rufipogon* OsRc (ABB17166); *Petunia hybrida* PhAN1 (AAG25928) and PhJAF13 (AAC39455); *Lilium hybrid* LhbHLH2 (BAE20058); *Antirrhinum majus* AmDEL (AAA32663.1); *Ipomoea nil* InDEL(BAE94393.1); *Dahlia pinnata* DvIVS (BAJ33516.1); *Ipomoea tricolor* ItbHLH2 (BAD18984.1); *Allium cepa* AcB2 (AUG71567); and *Zea mays* ZmR (P13027)

The secondary structure of the PdbHLH57 protein was further predicted using PSIPRED software (Fig. 2a). The results indicated that PdbHLH57 protein included 52.55% random coil, 37.42% alpha-helix, and 10.03% extended strand, with the highest number of random coil secondary structures. To better understand the functions of the PdbHLH57 protein, the tertiary structure was predicted with Phyre2 software (Fig. 2b). Through homology comparison analysis, the crystal structure of transcription factor egl3 was used as a template. 256 residues could be modeled at >90% confidence using multiple templates, indicating that the simulated tertiary structure of PdbHLH57 protein can be reliably predicted.

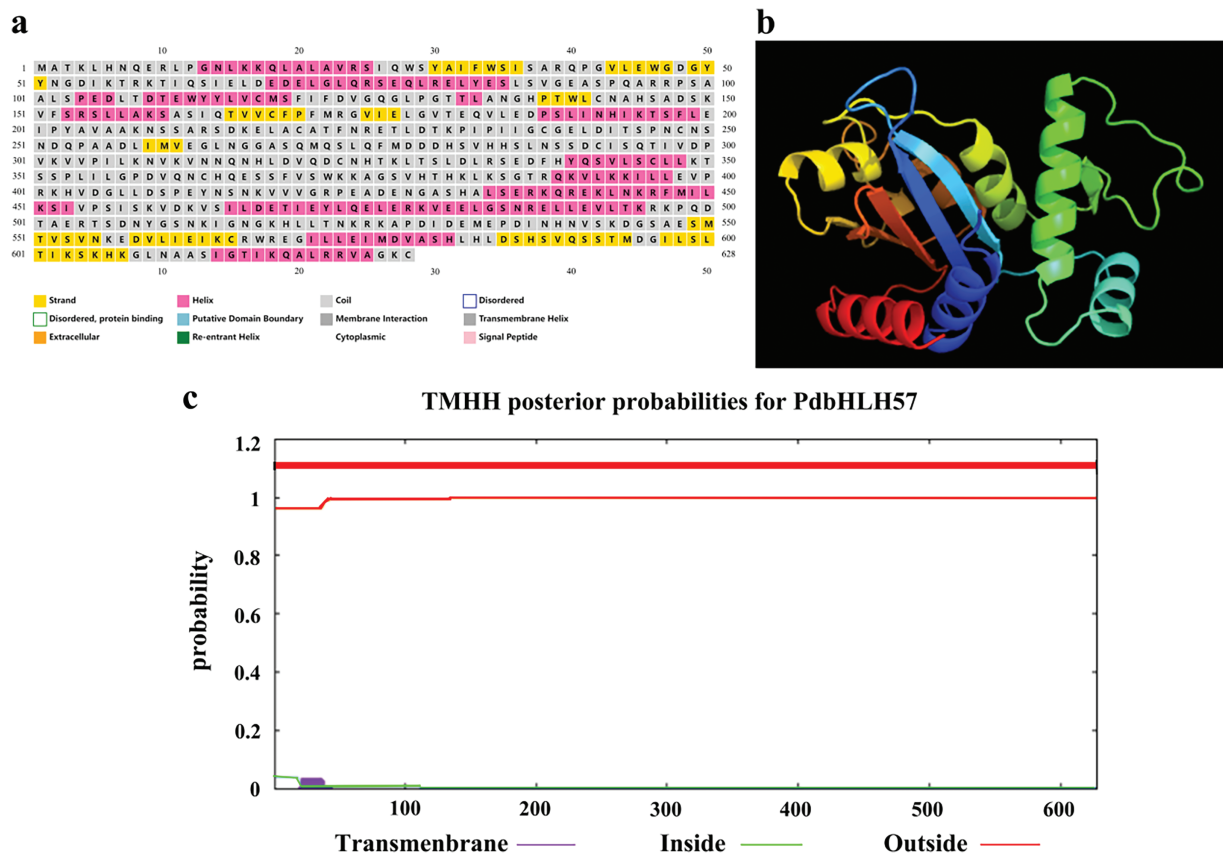


Figure 2: The prediction of the structure for PdbHLH57. (a) The prediction of secondary structure. (b) The prediction of tertiary structure. (c) Prediction of transmembrane structure in protein PdbHLH57

Furthermore, the transmembrane helices in protein PdbHLH57 were also predicted by TMHMM (Fig. 2c). The results showed that the first 60 AAs Exp number, AAs in TMHs Exp number, the predicted TMHs number is 0, 0.71, and 0.63, respectively, indicating that PdbHLH57 does not contain a transmembrane domain.

The prediction of the interaction network associated with PdbHLH57 was conducted with STRING. In the present study, PtrGL3 from *Populus trichocarpa*, homologous to PdbHLH57, was used to be a key node to predict the interaction network between PdbHLH57 and the corresponding proteins (Fig. S2). PdbHLH57 was predicted to form an interaction network with multiple proteins, including MYB-LIKE, WD-REPEAT, and bHLH92 (Table S2). Functional annotations of the PdbHLH57 were inferred from the known biological functions of proteins, providing some references for the prediction of potential functions of PdbHLH57 in color-leaf poplar.

3.2 Subcellular Localization Analysis and Transcriptional Activation Detection for *PdbHLH57*

To figure out the subcellular localization of the *PdbHLH57* protein, the CELLO online tools were first used to predict. When *PdbHLH57* protein is localized in the nucleus, the predicted score was 3.717, much higher than that for other locations (<0.8), indicating that *PdbHLH57* is localized in the nucleus. To further verify the subcellular localization of *PdbHLH57* protein through experiment, the fused vector containing green fluorescent protein and coding sequence of *PdbHLH57* was constructed and transiently expressed in 'ZSCY' protoplasts to confirm its subcellular localization. The PAN580-GFP was used as a control. There was a ubiquitous distribution for the fluorescence signal of 35S:GFP protein, whereas there was a specific distribution localized to the cell nucleus for the fluorescence signal of PAN580-*PdbHLH57*-GFP (Fig. 3), which further indicated that *PdbHLH57* was a nuclear protein.

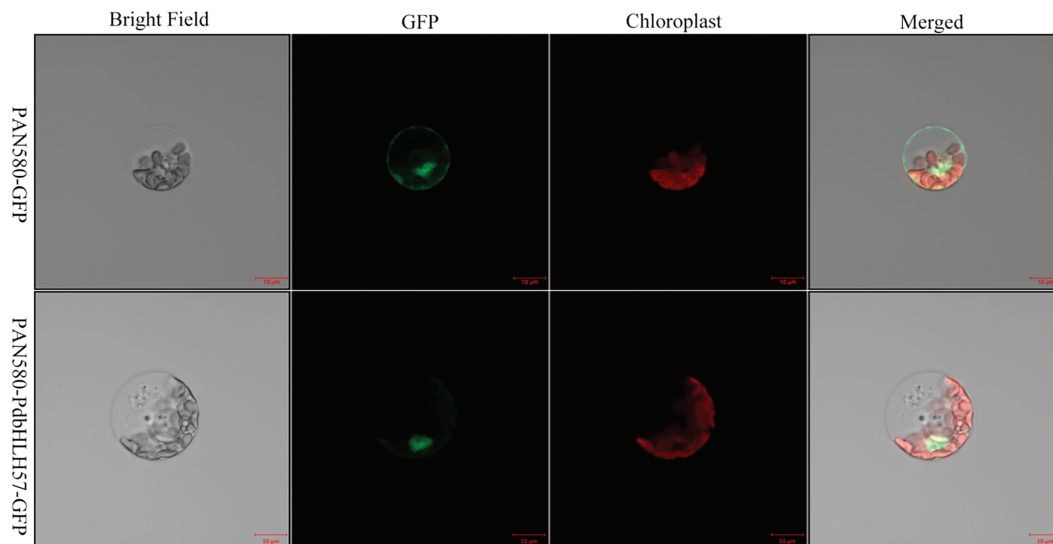


Figure 3: Subcellular localization of *PdbHLH57* protein. The vector PAN580-*PdbHLH57*-GFP or PAN580-GFP was incubated in the protoplasts of the 'ZSCY' leaf. The red and green fluorescence were excited and visualized with 488 and 561 nm lasers, respectively

To better explore the functions of *PdbHLH57*, the transactivation activity of *PdbHLH57* was detected in Y2H yeast cells with Y2H assays (Fig. 4). Compared with the negative and positive control, the transformed yeast cells containing pGBKT7-*PdbHLH57* can grow well under the selection medium, indicating that *PdbHLH57* exhibited self-transactivation activity (Fig. 4b). Two truncated variants were divided to further explore which part of *PdbHLH57* had transcriptional transactivation (Fig. 4a). Compared with the negative and positive control, the transformed yeast cells containing pGBKT7-*PdbHLH57*-1 can grow well under selection medium, and the yeast cells containing pGBKT7-*PdbHLH57*-2 cannot grow well under selection medium, indicating that *PdbHLH57*-1 had a self-transactivation activity, and *PdbHLH57*-2 can be used to construct the yeast two-hybrid cDNA library to further screen the proteins interacted with *PdbHLH57* (Fig. 4c).

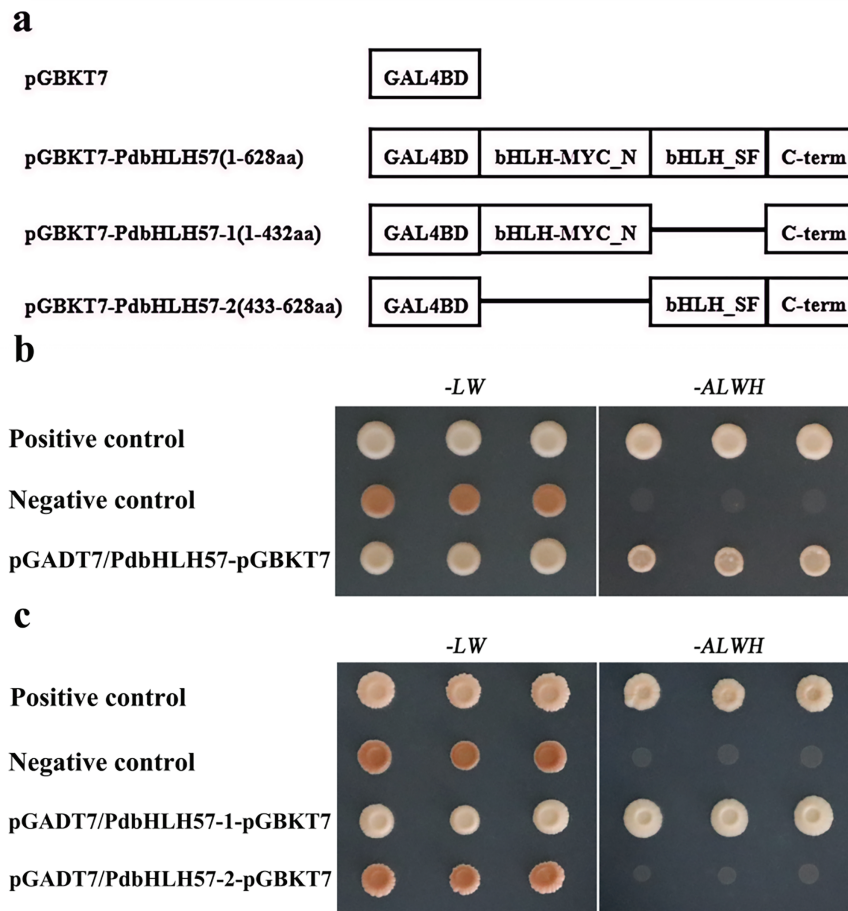


Figure 4: Self-activation test of PdbHLH57 protein in yeast. PdbHLH57-1(1-432aa). PdbHLH57-2 (433-628aa). pGADT7-largeT/pGBKT7-p53 (Positive control); pGADT7-largeT/pGBKT7-laminC (Negative control); SD-ALWH: -ade, -his, -leu, -trp; SD-LW: -leu, -trp

3.3 Expression Analysis of PdbHLH57 among Different Development Stages in the Leaves of 'ZSCY'

To better explore the roles of *PdbHLH57* in the leaves of 'ZSCY', the expression levels of *PdbHLH57* among different development stages were evaluated by qRT-PCR analysis (Fig. 5a). The expression level of *PdbHLH57* increased significantly from April to June, and decreased significantly continuously from June to October, indicating that *PdbHLH57* may play an important role at different developmental stages. As *PdbHLH57* might regulate anthocyanin biosynthesis (Fig. 1), the total anthocyanin contents of leaves from 'ZSCY' leaves at four different development stages were also conducted. The total anthocyanin content decreased significantly from April to June, increased significantly from June to August, and decreased significantly from August to October (Fig. 5b). The above results indicated that *PdbHLH57* might partially participate in the anthocyanin biosynthesis.

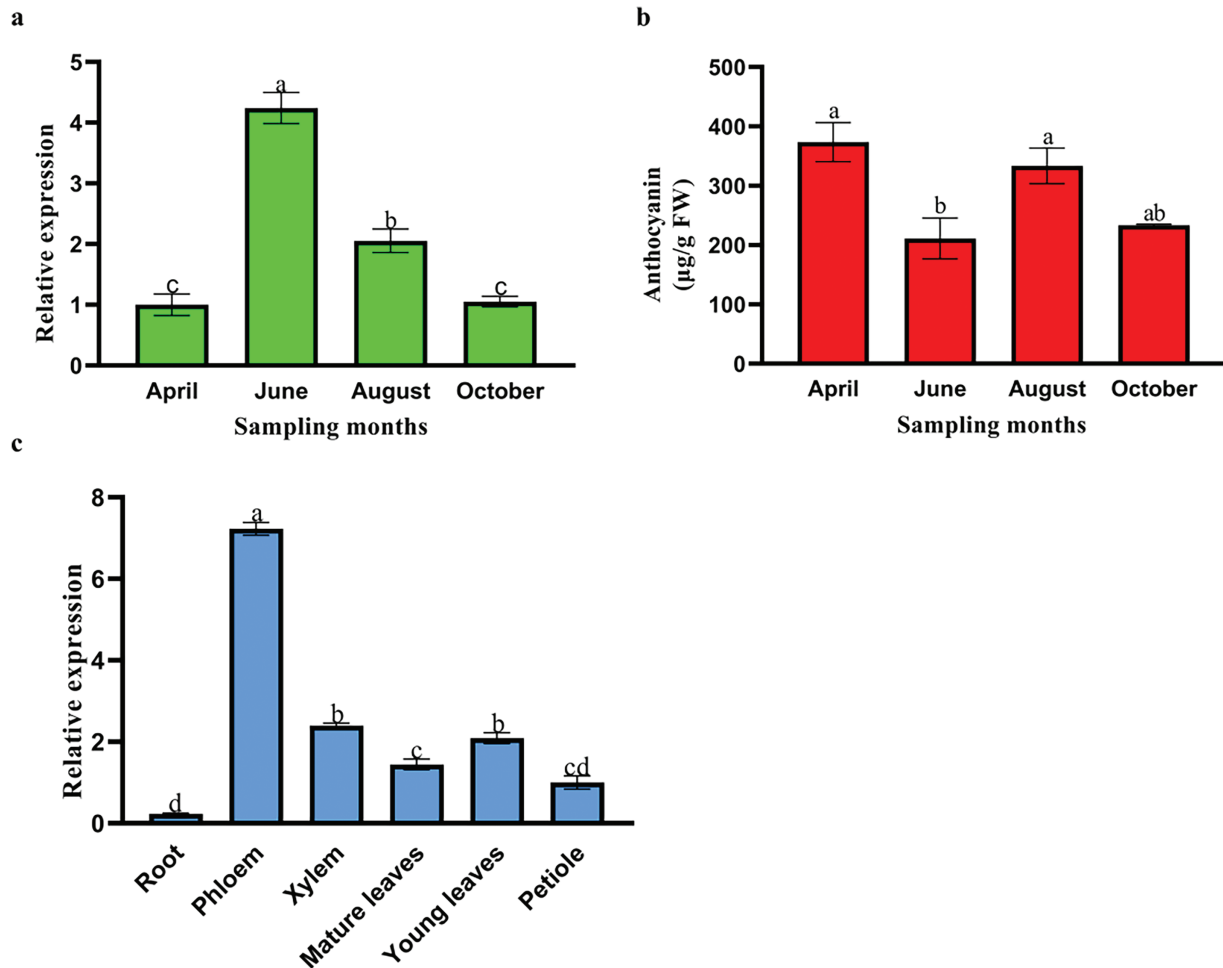


Figure 5: The expression levels of *PdbHLH57* among different development stages (a). The total anthocyanin contents of leaves from ‘ZSCY’ leaves at four different development stages (b). Spatial expression pattern of *PdbHLH57* in ‘ZSCY’ (c). The expression levels of *PdbHLH57* in different organs: young leaves, mature leaves, petioles, phloem, xylem, and roots. Different letters show significant differences with Duncan tests ($p < 0.05$), and error bars represent standard deviations

3.4 Spatial Expression Pattern of *PdbHLH57* in ‘ZSCY’

The function of genes is usually reflected through their expression patterns. To characterize the spatial expression pattern of *PdbHLH57* in ‘ZSCY’, the expression level of *PdbHLH57* was evaluated in different tissues, including xylem, mature leaves, young leaves, petioles, phloem, and roots (Fig. 5c). The expression of *PdbHLH57* can be detected among all the tissues of ‘ZSCY’ with different transcription levels. For example, there was a highest expression level for *PdbHLH57* in phloem, and a lowest expression level in roots, which has a 31.12 times difference in the expression level of *PdbHLH57* between phloem and roots. While no significant difference was observed among young leaves, mature leaves, and xylem for the expression level of *PdbHLH57* in ‘ZSCY’. The above results showed that *PdbHLH57* may exert various roles in different tissues of ‘ZSCY’.

4 Discussion

The bHLH family genes are involved in plant growth and development, which include the biosynthesis of anthocyanin. Although some researchers have reported the influences of bHLH genes on anthocyanin biosynthesis, our understanding of this topic in poplar remains limited. In present results, *PdbHLH57*, closely related to *AtGL3*, and *AtEGL3*, belongs to the bHLH IIIf subfamily (Fig. 1). In previous studies, most anthocyanin biosynthesis-related bHLH transcription factors belong to the bHLH IIIf subfamily. *PhJAF13*, *AtEGL3*, and *AtGL3* have also been reported to participate in the biosynthesis of anthocyanin [23–25]. *MdbHLH3*, isolated from apple (*Malus domestica* Borkh.), promoted the accumulation of anthocyanin and the coloration of fruit under low temperatures [13]. *MdbHLH33* could reduce the inhibitory effect of *MdMYB16* on the biosynthesis of anthocyanin by interacting with *MdMYB16* [26]. In grapevine (*Vitis vinifera*), *VvMYC1* physically interacted with *MYBPA1*, *MYBA1/A2*, *MYB5b*, and *MYB5a*, could regulate gene expression, and enhance their proanthocyanidin and/or anthocyanin accumulation [27]. Combined with our results, *PdbHLH57* might play an important role in anthocyanin synthesis.

To explore the functions of transcription factors, it is essential to verify whether a transcription factor has self-activation activity or not. Some bHLH transcription factors have been reported to show self-activation activity. For example, in tomato, there was a self-activation activity for *SlbHLH96*, and no self-activation activity for C-terminal segments of *SlbHLH96* (200–441 bp), which include the conserved bHLH domain [28]. However, other transcription factors do not have self-activation activity. *CmbHLH2* from Chrysanthemums (*Chrysanthemum morifolium* Ramat.) and *AcB2* from onion (*Allium cepa* L.) showed no self-activation activity [14,16]. In our results, there was a self-activation activity for *PdbHLH57*, and no self-activation activity for C-terminal segments of *PdbHLH57* (*PdbHLH57-2*, 426–628) with conserved bHLH domain, which can be used for its functional identification.

Various spatial expression patterns occurred for bHLH genes in different plant species. In *Solanum lycopersicum*, *SlbHLH041* was expressed at a higher level in leaves than in other organs [29]. The expression of *GhPAS1* in *Gossypium* spp. occurred in various tissues, with a preference for leaves [30]. In eggplant (*Solanum melongena* L.), bHLH genes exhibited diverse spatial expression patterns. *SmbHLH1* was expressed highly in the flowers, petioles, leaves, and peels of purple-peel eggplant, but lower in green and white tissues. Conversely, *SmbHLH117* was more highly expressed in green tissues like stems and leaves, but less in flowers and peels [31]. In *Prunus mume*, several bHLH Ib (2) subfamily genes had higher expression levels in roots, while *PmbHLH58* and *PmbHLH33* were expressed much higher in stems and leaves, respectively, indicating that the gene function in the same family gradually diverged during the evolutionary process [32]. In the present study, *PdbHLH57* was expressed significantly higher in the phloem than in other tissues, suggesting that *PdbHLH57* may regulate the growth and development of ‘ZSCY’ special in the phloem tissue.

Different bHLH genes have various expression patterns at different developmental stages in plants. For example, the contents of anthocyanin in *Malus hupehensis* increased from the flower developmental stage S1 to S2 and decreased from S2 to S3. The expression levels of some genes associated with anthocyanin synthesis (*PAL*, *CHI*, *CHS*, *FLS*) had a similar pattern from S1 to S3, while the expression level of *MYB* always increased from S1 to S3, which is inconsistent with the changes of anthocyanin contents [33]. In Chinese bayberry, the anthocyanin contents increased continuously at different fruit development (78, 82, and 86 days after full bloom). The expression level of *MrbHLH1* increased from 78 days after full bloom to 82 days after full bloom, and decreased from 82 days after full bloom to 86 days after full bloom, while the expression level of *MrMYB1* increased continuously at different fruit development [34]. In blueberries, anthocyanin contents continuously increased during fruit development stages, while the expression level of *VcbHLH1-2* declined from the green to the red stage and increased from red to blue stages, which is inconsistent with the changes in anthocyanin contents [35]. LibHLH members of the same subfamily (XII

subfamily) have different expression patterns in *Lagerstroemia indica*, such as *LibHLH45*, *LibHLH50*, and *LibHLH62*, indicating that LibHLH members have diverse expression patterns, and might play a role in the synthesis of anthocyanin [36]. In the present results, the expression pattern of *PdbHLH57* in ‘ZSCY’ leaves was inconsistent with the accumulation of anthocyanin (Fig. 5), indicating that *PdbHLH57* might partially regulate anthocyanin biosynthesis.

5 Conclusion

In the present study, a *PdbHLH57* gene, belonging to the IIIf group of bHLH, was characterized, which was isolated and cloned from the colored-leaf poplar ‘ZSCY’. *PdbHLH57* protein was localized to the nucleus in the leaf protoplasts of ‘ZSCY’ according to subcellular localization analysis. *PdbHLH57-2* (433-628aa) lacked transcription activation, which can be utilized to construct a yeast two-hybrid cDNA library for further screening of proteins that interact with *PdbHLH57*. The expression levels of different developmental stages and spatial patterns of *PdbHLH57* in ‘ZSCY’ were also evaluated, which indicated its potential characteristics. The findings of the present work provided references for further functional identification of *PdbHLH57* in colored-leaf poplar.

Acknowledgement: Not applicable.

Funding Statement: This research was supported by the Natural Science Foundation of Jiangsu Province, China (BK20242007), the Natural Science Foundation of China (32271916), and the Jiangsu Agricultural Science and Technology Innovation Fund [CX(24)3048].

Author Contributions: The authors confirm their contributions to the paper as follows: study conception and design: Weibing Zhuang and Zhong Wang; data collection: Yuhang Li, Xiaochun Shu and Li Sun; analysis and interpretation of results: Yuhang Li, Tao Wang and Tengyue Yan; draft manuscript preparation: Yuhang Li; writing—review and editing: Zhihong Gao, Bingjun Yu, Weibing Zhuang and Zhong Wang. All authors reviewed the results and approved the final version of the manuscript.

Availability of Data and Materials: This article included all the data and materials.

Ethics Approval: Not applicable.

Conflicts of Interest: The authors declare no conflicts of interest to report regarding the present study.

Supplementary Materials: The supplementary material is available online at <https://doi.org/10.32604/phyton.2025.063647>.

References

1. Zhang F, Wan XQ, Zheng YX, Sun LX, Chen QB, Guo YL, et al. Physiological and related anthocyanin biosynthesis genes responses induced by cadmium stress in a new colored-leaf plant “Quanhong Poplar”. *Agrofor Syst.* 2014;88(2):343–55. doi:10.1007/s10457-014-9687-4.
2. Chen MJ, Li H, Zhang W, Huang L, Zhu J. Transcriptomic analysis of the differences in leaf color formation during stage transitions in *Populus × euramericana* ‘Zhonghuahongye’. *Agronomy.* 2022;12(10):2396. doi:10.3390/agronomy12102396.
3. Chen MJ, Chang CF, Li H, Huang L, Zhou ZS, Zhu J, et al. Metabolome analysis reveals flavonoid changes during the leaf color transition in *Populus × euramericana* ‘Zhonghuahongye’. *Front Plant Sci.* 2023;14:1162893. doi:10.3389/fpls.2023.1162893.
4. Zhu YL, Wang N, Cheng XJ, Zhou CS. A new poplar red foliar variety ‘Quanhong’. *Sci Silvae Sin.* 2012;48(2):188.
5. Zhu YL, Cheng XJ. A new poplar red foliar variety ‘Zhonghong’. *Sci Silvae Sin.* 2008;44(10):173–4.

6. Zhuang WB, Shu XC, Lu XY, Wang T, Zhang FJ, Wang N, et al. Ornamental poplar ‘Zhongshancai Yun’. HortScience. 2021;56(10):1291–2. doi:10.21273/HORTSCI16016-21.
7. Toledo-Ortiz G, Huq E, Quail PH. The Arabidopsis basic/helix-loop-helix transcription factor family. Plant Cell. 2003;15(8):1749–70. doi:10.1105/tpc.013839.
8. Heim MA. The basic helix-loop-helix transcription factor family in plants: a genome-wide study of protein structure and functional diversity. Mol Biol Evol. 2003;20(5):735–47. doi:10.1093/molbev/msg088.
9. Li M, Sun L, Gu H, Cheng D, Guo X, Chen R, et al. Genome-wide characterization and analysis of bHLH transcription factors related to anthocyanin biosynthesis in spine grapes (*Vitis davidii*). Sci Rep. 2021;11(1):6863. doi:10.1038/s41598-021-85754-w.
10. Baudry A, Heim MA, Dubreucq B, Caboche M, Weisshaar B, Lepiniec L. TT2, TT8, and TTG1 synergistically specify the expression of *BANYULS* and proanthocyanidin biosynthesis in *Arabidopsis thaliana*. Plant J. 2004;39(3):366–80. doi:10.1111/j.1365-313X.2004.02138.x.
11. Ludwig SR, Habera LF, Dellaporta SL, Wessler S. Lc, a member of the maize R gene family responsible for tissue-specific anthocyanin production, encodes a protein similar to transcriptional activators and contains the myc-homology region. Proc Natl Acad Sci. 1989;86(18):7092–96. doi:10.1073/pnas.86.18.7092.
12. Nakatsuka A, Yamagishi M, Nakano M, Tasaki K, Kobayashi N. Light-induced expression of basic helix-loop-helix genes involved in anthocyanin biosynthesis in flowers and leaves of Asiatic hybrid lily. Sci Hort. 2009;121(1):84–91. doi:10.1016/j.scienta.2009.01.008.
13. Xie XB, Li S, Zhang RF, Zhao J, Chen YC, Zhao Q, et al. The bHLH transcription factor *MdbHLH3* promotes anthocyanin accumulation and fruit colouration in response to low temperature in apples. Plant Cell Env. 2012;35(11):1884–97. doi:10.1111/j.1365-3040.2012.02523.x.
14. Xiang LL, Liu XF, Li X, Yin XR, Grierson D, Li F, et al. A novel bHLH transcription factor involved in regulating anthocyanin biosynthesis in Chrysanthemums (*Chrysanthemum morifolium* Ramat.). PLoS One. 2015;10(11):e0143892. doi:10.1371/journal.pone.0143892.
15. Song M, Wang H, Wang Z, Huang H, Chen S, Ma H. Genome-wide characterization and analysis of bHLH transcription factors related to anthocyanin biosynthesis in Fig (*Ficus carica* L.). Front Plant Sci. 2021;12:730692. doi:10.3389/fpls.2021.730692.
16. Li X, Cao L, Jiao B, Yang H, Ma C, Liang Y. The bHLH transcription factor AcB2 regulates anthocyanin biosynthesis in onion (*Allium cepa* L.). Hort. 2022;9:uhac128. doi:10.1093/hr/uhac128.
17. Wang H, Wang X, Yu C, Wang C, Jin Y, Zhang H. MYB transcription factor PdMYB118 directly interacts with bHLH transcription factor PdTT8 to regulate wound-induced anthocyanin biosynthesis in poplar. BMC Plant Biol. 2020;20(1):173. doi:10.1186/s12870-020-02389-1.
18. Wan S, Li C, Ma X, Luo K. PtrMYB57 contributes to the negative regulation of anthocyanin and proanthocyanidin biosynthesis in poplar. Plant Cell Rep. 2017;36(8):1263–76. doi:10.1007/s00299-017-2151-y.
19. Wang XJ, Peng XQ, Shu XC, Li YH, Wang Z, Zhuang WB. Genome-wide identification and characterization of *PdbHLH* transcription factors related to anthocyanin biosynthesis in colored-leaf poplar (*Populus deltoids*). BMC Genomics. 2022;23(1):244. doi:10.1186/s12864-022-08460-5.
20. Yang P, Sun Y, Sun X, Li Y, Wang L. Optimization of preparation and transformation of protoplasts from *Populus simonii* × *P. nigra* leaves and subcellular localization of the major latex protein 328 (MLP328). Plant Methods. 2024;20(1):3. doi:10.1186/s13007-023-01128-5.
21. Zhuang WB, Wang HX, Liu TY, Wang T, Zhang FJ, Shu XC, et al. Integrated physiological and genomic analysis reveals structural variations and expression patterns of candidate genes for colored- and green-leaf poplar. Sci Rep. 2019;9(1):11150. doi:10.1038/s41598-019-47681-9.
22. Wang S, Yao W, Wei H, Jiang T, Zhou B. Expression patterns of ERF genes underlying abiotic stresses in di-haploid *Populus simonii* × *P. nigra*. Sci World J. 2014;2014:1–10.
23. Tominaga-Wada R, Masakane A, Wada T. Effect of phosphate deficiency-induced anthocyanin accumulation on the expression of *Solanum lycopersicum* *GLABRA3* (*SIGL3*) in tomato. Plant Signal Behav. 2018;13(6):e1477907. doi:10.1080/15592324.2018.1477907.

24. Chiu LW, Li L. Characterization of the regulatory network of *BoMYB2* in controlling anthocyanin biosynthesis in purple cauliflower. *Planta*. 2012;236(4):1153–64. doi:10.1007/s00425-012-1665-3.
25. D'Amelia V, Aversano R, Batelli G, Caruso I, Castellano MM, Castro-Sanz AB, et al. High *ANI* variability and interaction with basic helix-loop-helix co-factors related to anthocyanin biosynthesis in potato leaves. *Plant J*. 2014;80(3):527–40. doi:10.1111/tpj.12653.
26. Xu H, Wang N, Liu J, Qu C, Wang Y, Jiang S, et al. The molecular mechanism underlying anthocyanin metabolism in apple using the *MdMYB16* and *MdbHLLH33* genes. *Plant Mol Biol*. 2017;94(1–2):149–65. doi:10.1007/s11103-017-0601-0.
27. Hichri I, Heppel SC, Pillet J, Leon C, Czemmel S, Delrot S, et al. The basic helix-loop-helix transcription factor *MYC1* is involved in the regulation of the flavonoid biosynthesis pathway in grapevine. *Mol Plant*. 2010;3(3):509–23. doi:10.1093/mp/ssp118.
28. Liang Y, Ma F, Li B, Guo C, Hu T, Zhang M, et al. A bHLH transcription factor, *SlbHLLH96*, promotes drought tolerance in tomato. *Hortic Res*. 2022;9:uhac198. doi:10.1093/hr/uhac198.
29. Sun H, Fan HJ, Ling HQ. Genome-wide identification and characterization of the *bHLLH* gene family in tomato. *BMC Genomics*. 2015;16(1):9. doi:10.1186/s12864-014-1209-2.
30. Wu H, Ren Z, Zheng L, Guo M, Yang J, Hou L, et al. The bHLH transcription factor *GhPAS1* mediates BR signaling to regulate plant development and architecture in cotton. *Crop J*. 2021;9(5):1049–59. doi:10.1016/j.cj.2020.10.014.
31. Tian S, Li L, Wei M, Yang F. Genome-wide analysis of basic helix-loop-helix superfamily members related to anthocyanin biosynthesis in eggplant (*Solanum melongena* L.). *PeerJ*. 2019;7:e7768. doi:10.7717/peerj.7768.
32. Ding A, Ding A, Li P, Wang J, Cheng T, Bao F, et al. Genome-wide identification and low-temperature expression analysis of bHLH genes in *Prunus mume*. *Front Genet*. 2021;12:762135. doi:10.3389/fgene.2021.762135.
33. Zhang Y, Liu F, Wang B, Wu H, Wu J, Liu J, et al. Identification, characterization and expression analysis of anthocyanin biosynthesis-related bHLH genes in Blueberry (*Vaccinium corymbosum* L.). *Int J Mol Sci*. 2021;22(24):13274. doi:10.3390/ijms222413274.
34. Liu XF, Yin XR, Allan AC, Lin WK, Shi YN, Huang YJ, et al. The role of *MrbHLLH1* and *MrMYB1* in regulating anthocyanin biosynthetic genes in tobacco and Chinese bayberry (*Myrica rubra*) during anthocyanin biosynthesis. *Plant Cell Tissue Organ Cult*. 2013;115(3):285–98. doi:10.1007/s11240-013-0361-8.
35. Han M, Yang C, Zhou J, Zhu J, Meng J, Shen T, et al. Analysis of flavonoids and anthocyanin biosynthesis-related genes expression reveals the mechanism of petal color fading of *Malus hupehensis* (Rosaceae). *Braz J Bot*. 2020;43(1):81–9. doi:10.1007/s40415-020-00590-y.
36. Yu M, Bai M, Chen M, Zhang G, Zhao Y, Ma Q, et al. Identification of bHLH transcription factors and screening of anthocyanin-related genes in *Lagerstroemia indica*. *Genetica*. 2024;152(4–6):179–97. doi:10.1007/s10709-024-00215-2.